CrystEngComm

ROYAL SOCIETY OF CHEMISTRY

PAPER

View Article Online
View Journal | View Issue

Cite this: *CrystEngComm*, 2025, **27**, 5356

A DSC study of the non-isothermal cold crystallization and relaxation effects in ubiquinone and ubiquinol†

Rafael Barbas, [a] Lídia Bofill,[b] Dafne de Sande [a] and Rafel Prohens *[c]

Received 3rd April 2025,
Accepted 3rd July 2025

DOI: 10.1039/d5ce00368g

rsc.li/crystengcomm

Cold crystallization effects, the kinetics-dependent crystallization behaviour of amorphous ubiquinone and ubiquinol produced in a series of quenching from-the-melt experiments, have been extensively studied through the combination of differential scanning calorimetry (DSC) and powder X-ray diffraction (PXRD) techniques under a big diversity of experimental conditions, which has allowed the exploration of their poorly understood polymorphic landscapes. The investigation revealed the existence of a non-previously described polymorph together with a rich set of kinetically dependent transformations, which were observed for the first time by thermal analysis conducted at different heating rates in both oxidized and reduced solid forms of Coenzyme Q10.

Introduction

Crystal polymorphism, defined as the ability of a substance to exist as two or more crystalline phases with different arrangements of the molecule in the crystal lattice,[1] is one of the most intensively studied phenomena in the field of solid-state chemistry due to its almost ubiquitous occurrence, with more than 80% of organic compounds having been described as polymorphic.[2] It affects a plethora of compounds, and the safety and regulatory issues that may involve new polymorphs of an ingredient for human consumption require a thorough knowledge of its polymorphism before or during its development. However, polymorphism is not a rigid concept and several variations exist, not without some controversial implications like in the case of isostructurality, a term defined by Fabian and Kalman as the similarity of the spatial arrangements of the molecules of different compounds in their crystals,[3] which when applied to polymorphs of the same compound can provide an explanation to another phenomenon as the concomitant polymorphism.[4] Moreover, different polymorphs of an organic compound showing very similar physical properties and crystal packing have been described as "quasi-isostructural".[5] Cold crystallization is a unique phenomenon where compounds crystallize during heating rather than cooling. Usually, chemical compounds transform from solids to liquids above their melting point and revert to solids upon cooling. However, cold crystallization involves an exothermic phase transition from an amorphous to a crystalline state during heating. Differential scanning calorimetry (DSC) analysis shows that, in some cases, the liquid state can reach a deep supercooled state without crystallization during cooling through quenching from the melt. Further cold crystallization occurs *via* glass transition upon subsequent heating. This process is commonly observed in polymer-based systems[6,7] but is rare in small molecules.[8–10] In this context, DSC is a technique frequently used in the study of crystalline polymorphism, as it allows for the combination of different heating and cooling programs that influence the crystallization phenomenon and the search for new metastable polymorphs.[11]

Ubiquinone (Coenzyme Q10, CoQ10) is an endogenous lipophilic benzoquinone and a vital component of aerobic cellular respiration. In mitochondria, CoQ10 is a key component of the respiratory chain for adenosine triphosphate synthesis, and it is found in both the reduced and oxidized states, in plants and animals. Although endogenous synthesis occurs under physiological conditions, its efficiency decreases with age, which recommends supplementation in order to achieve health benefits related to blood pressure, cognitive function or insulin resistance,[12] and it has been reported recently that CoQ10 supplementation might have beneficial effects on glycemic control, especially in diabetic patients.[13] Ubiquinol is the reduced form of CoQ10 and it is a lipid-soluble antioxidant that plays an intrinsic role in protecting circulating lipoproteins against oxidative damage and in protecting

[a] *Unitat de Polimorfisme i Calorimetria, Centres Científics i Tecnològics, Universitat de Barcelona, Baldiri Reixac 10, 08028 Barcelona, Spain*
[b] *CIRCE Scientific, Parc Científic de Barcelona, Baldiri Reixac 4-12, 08028 Barcelona, Spain*
[c] *Laboratory of Organic Chemistry, Faculty of Pharmacy and Food Sciences, University of Barcelona, Avda. Joan XXIII, 08028 Barcelona, Spain. E-mail: rafel_prohens@ub.edu*

† Electronic supplementary information (ESI) available: Detailed analysis conditions and NMR, DSC, TGA, and PXRD diagrams, Fig. S1 to S24. See DOI: https://doi.org/10.1039/d5ce00368g

mitochondria and other cellular components from reactive oxygen species generated during mitochondrial respiration. It has been claimed, not without some controversy,[14] that ubiquinol is more bioavailable than ubiquinone, which is why there has been an interest in stable formulations of ubiquinol, such as gel encapsulation[15] or cocrystallization.[16] However, in spite of the existence of a number of scientific studies covering different topics on the solid-state stability of coenzyme Q10, not much is known about the transformations between the potential solid-state forms that can occur when amorphous forms are produced and then recrystallized. The polymorphism of ubiquinone and ubiquinol has been studied in the past by means of DSC. In particular, the work by Katsikas and Quinn,[17] which was also devoted to study the lower homologues of ubiquinone, showed that two different solid forms of ubiquinone (named Q^{C1} and Q^{C2}) can be obtained from the liquid phase by using rapid or slow cooling rates through a complex series of thermotropic events. However, the description of this transformation is partial. Moreover, since both compounds have long-chain conformationally flexible substituents in their structures, it is expected that a high incidence of polymorphism will be observed, since it is well known that conformational flexibility plays an important role in crystallization.[18] Some previously studied compounds like, for instance, the *n*-alkane series[19] and calixarenes[20] show a large number of polymorphs explained by the flexibility of their substituents and a subtle balance of strong intra and intermolecular H-bond interactions. In this work, we report the polymorphic behaviour using DSC when solid ubiquinone and ubiquinol are quenched from the melt, which suggests the existence of a continuum-like set of conformational polymorphs in both compounds. Our work provides evidence of non-previously described polymorphs of two natural products of great relevance to the human body, enriching the scarce collection of thermal analysis data available in the literature related to kinetically dependent polymorphic transformations (Scheme 1).

Materials and methods

Materials

Ubiquinone (form B) (>99%) and ubiquinol (form B) (>99%) used in this study were used as received from BOC Sciences. Preparation of ubiquinol (form A): ubiquinol form B (500 mg, 0.578 mmol) was suspended in ACN (50 mL) at 25 °C and it was stirred overnight. The solid was filtered and dried under vacuum for 24 hours.

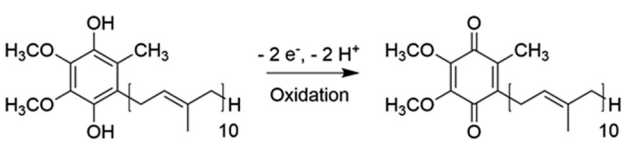

Scheme 1 Chemical structure of ubiquinol and its oxidized form ubiquinone.

Differential scanning calorimetry (DSC)

Differential scanning calorimetry analysis was carried out using Mettler–Toledo DSC-822e and DSC-30 calorimeters. Experimental conditions: aluminum crucibles of 40 μL volume, an atmosphere of dry nitrogen with a 50 mL min^{-1} flow rate, and variable heating rates (see the ESI† for further details, refer to section 1.1). The calorimeters were calibrated with indium of 99.99% purity (DSC-822e: m.p.: 156.6 °C; ΔH: 28.31 J g^{-1} and DSC-30: m.p.: 156.8 °C; ΔH: 28.48 J g^{-1}). A Tau-lag adjustment was performed prior to measurements in order to correct the dynamic behaviour of the measuring cell.

Thermogravimetric analysis (TGA)

Thermogravimetric analysis was performed using a Mettler–Toledo TGA-851e thermobalance. Experimental conditions: alumina crucibles of 70 μL volume, an atmosphere of dry nitrogen with a 50 mL min^{-1} flow rate, and a heating rate of 10 °C min^{-1}.

X-ray powder diffraction analysis (XRPD)

X-ray powder diffraction patterns of ubiquinone and ubiquinol were measured on a PANalytical X'Pert PRO MPD (transmission configuration with Cu Kα radiation, λ = 1.5418 Å) with a focalizing elliptic mirror and a PIXcel detector, and a maximum active detector length of 3.347°. The transmission geometry configuration included a convergent beam with a focalizing mirror, a flat sample sandwiched between low absorbing films measuring from 1 to 40° in 2θ, a step size of 0.026°, and a measuring time of 30 min at 298 K. The experimental conditions for XRPD variable temperature analysis are detailed in the ESI† (refer to section 1.2).

Nuclear magnetic resonance (NMR)

Proton nuclear magnetic resonance (^{1}H-NMR) spectra were measured on a Varian Mercury 400 (400 MHz) spectrometer. Chemical shifts for protons are reported in parts per million (ppm) downfield from tetramethylsilane (TMS) and referenced to the residual proton signal in the NMR solvent (chloroform-*d*: δ 7.26). Experimental conditions: delay: 1 second; pulse: 45°; scans: 32.

Results and discussion

Polymorphism of ubiquinone

The first reference about the polymorphism of ubiquinone was reported in 1983, which described the melting point of form A at 43.80 °C with an associated heat of 101.00 J g^{-1} (original values reported: 316.8 K and 87.2 kJ mol^{-1})[17] and the second reference was reported in 2013, which described the melting point of form B at 49.35 °C with an associated heat of 130.66 J g^{-1} (original values reported: 322.35 K and 112.8 kJ mol^{-1}).[21] Both melting point values were obtained at a heating rate of 5 °C min^{-1}. Thus, it is inferred that forms A and B are monotropically related according to the heat-of-

fusion rule (Burger and Ramberger) since the higher enthalpy of fusion corresponds to the higher melting point form.[22]

Thermal analysis of CoQ10 quenched from the melt

With the initial aim to discover new polymorphs of the two forms of CoQ10 quenching from the melt experiments using DSC were performed. First, commercial powder ubiquinone (form B) was heated at 10 °C min^{-1} under dry nitrogen until 300 °C (Fig. S1†). Since no loss in weight after the melting of ubiquinone was observed by thermogravimetry (Fig. S2†), a quenching-from-the-melt experiment was conducted and the presence of the thermotropic transformations previously reported was observed (Fig. 1). Thus, once the liquid phase was quenched at −100 °C, the amorphous phase was produced, which showed a glass transition at −71.65 °C with a ΔC_p of 0.445 J g^{-1} K^{-1} when heated at 5 °C min^{-1}, followed by the mentioned consecutive endothermic/exothermic thermal events. In view of this behavior, we decided to study two stages according to Fig. 1: (1) cold crystallization from the amorphous phase below 0 °C at different heating rates and (2) endothermic/exothermic thermal events above 0 °C at different heating rates.

Stage 1: study of cold crystallization from the amorphous phase below 0 °C at different heating rates. In order to study the effect of cold crystallization from the amorphous phase, we registered DSC traces applying different cyclic methods at different heating rates after a common quenching-from-the-melt cooling rate program (Tables S1 and S2†). We started by applying different heating rates between −100 °C and 0 °C followed by a heating rate of 1 °C min^{-1} between 0 °C and 70 °C (see ESI† Table S1 and method B). The reason for using this low heating rate was to increase resolution in a region where several consecutive thermal events were present, (Fig. 1b). The use of different heating rates does not very much affect the first phenomenon around −75 °C (glass transition) but it does to the subsequent exothermic phenomenon (cold crystallization), which shifts from −53 °C to −27 °C between 0.5 °C min^{-1} and 50 °C min^{-1} heating rates. The glass transition is not a first-order phase transition, but a kinetic phenomenon,[23] in the same way as crystallization, which explains why they both shift to higher temperatures when increasing the heating rate (Fig. 2).

The consequence of varying heating rates below 0 °C is not only the expected shift of the onset associated with the cold crystallization from the amorphous phase but also the observation of different behaviors in the subsequent melting of the crystalline phase. Thus, at the same heating rate of 1 °C min^{-1} above 0 °C, the melting of the crystalline phase depends on the previous variable heating rate cold crystallization process. Two main different overlapped processes are observed (Fig. 3): one exothermic/endothermic/exothermic overlapped phenomena around 17 °C assigned to the crystalline rearrangement and subsequent melting of a new polymorph (named form C) followed by another endothermic/exothermic phenomenon at around 24 °C

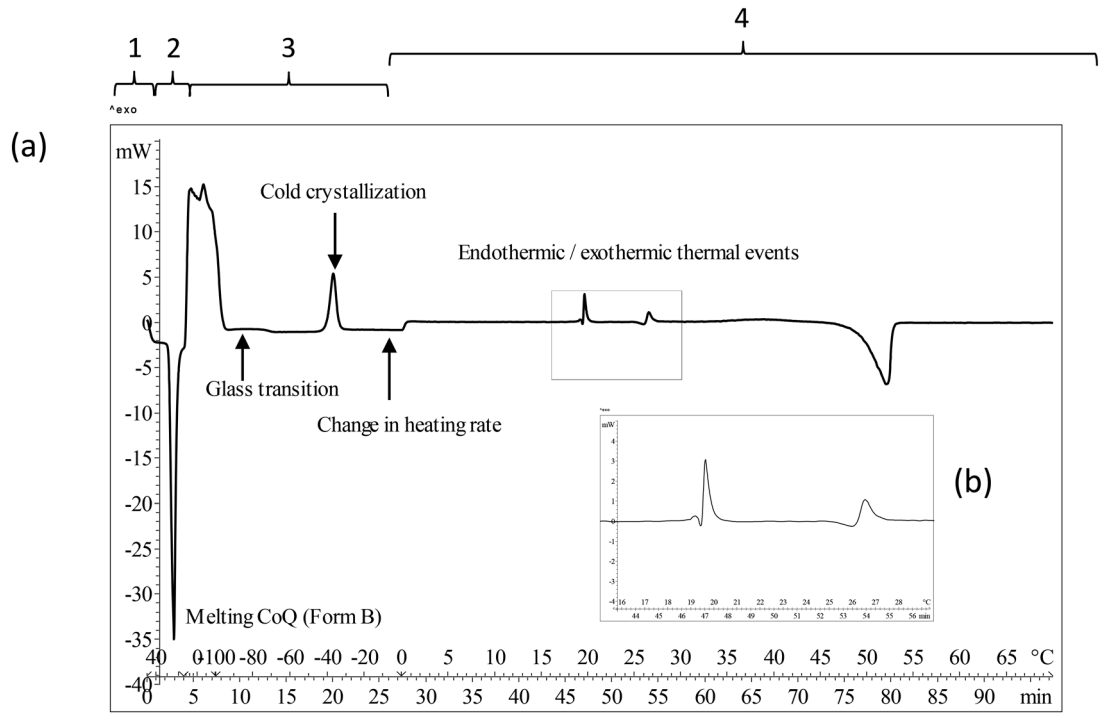

Fig. 1 (a) DSC thermogram of ubiquinone bulk powder quenching from the melt experiment corresponding to method B-4: step 1: heating from 30 °C to 70 °C at a rate of 10 °C min^{-1} followed by step 2: cooling from 70 °C to −100 °C at a rate of 50 °C min^{-1}, followed by step 3: heating from −100 °C to 0 °C at a rate of 5 °C min^{-1}, and finally, followed by step 4: heating from 0 °C to 70 °C at a rate of 1 °C min^{-1}. (b) Exothermic/endothermic/exothermic and endothermic/exothermic thermal events have been enlarged for clarity.

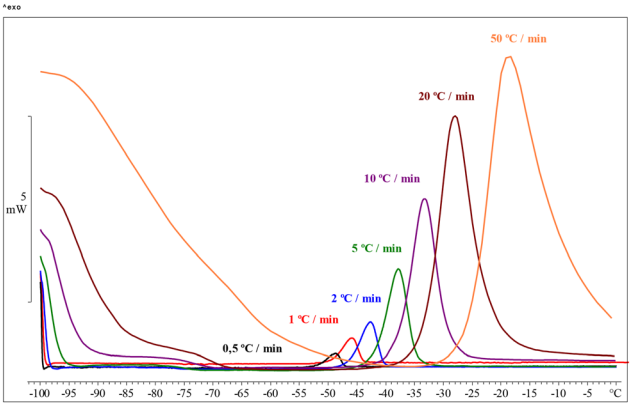

Fig. 2 Overlapping DSC thermograms of ubiquinone after quenching from the melt, from −100 °C to 0 °C at different heating rates (0.5, 1, 2, 5, 10, 20, and 50 °C min^{-1}) (method B, step 3).

assigned to the melting of the previously observed form by Katsikas and Quinn work[17] (named form D).

Subtle differences in each thermogram observed in Fig. 3 suggest that the different heating rates starting from the amorphous phase affect the subsequent cold crystallization events leading to the formation of diverse solid forms with slightly different molecular arrangements, which are nearly iso-energetic solid forms exhibiting very high degrees of similarity in physical properties. Afterwards, form D melts, recrystallizes and rearranges into form A through a broad exothermic phenomenon (from roughly 30 to 40 °C), finally melting at 46 °C (Fig. 4).

The exothermic phenomenon observed around 33 °C can be assigned to a crystallization or a thermal rearrangement. Aiming to get deeper insight into this phenomenon, two DSC experiments were carried out after the quenching-from-the-melt with a heating rate of 50 °C min^{-1} between −100 °C and 0 °C and a heating rate of 1 °C min^{-1} between 0 °C and 28 °C (1st experiment) and between 0 °C and 40 °C (2nd experiment). The samples were gently removed from the DSC

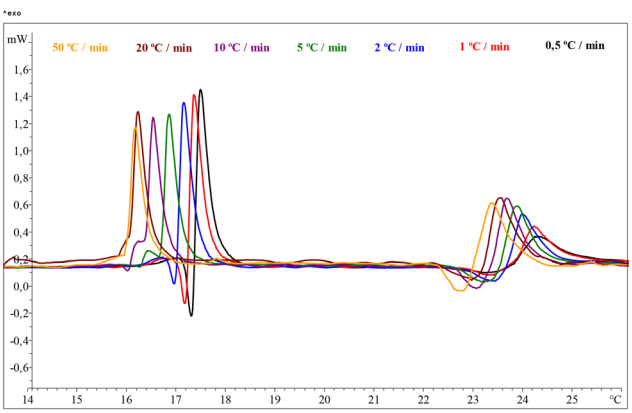

Fig. 3 Overlapping DSC thermograms of ubiquinone at a heating rate of 1 °C min^{-1} from 0 °C to 70 °C (method B, step 4). The heating rates of the previous cold crystallization step (Fig. 2) are shown in the figure for clarity. Enlarged view from 14 °C to 26 °C.

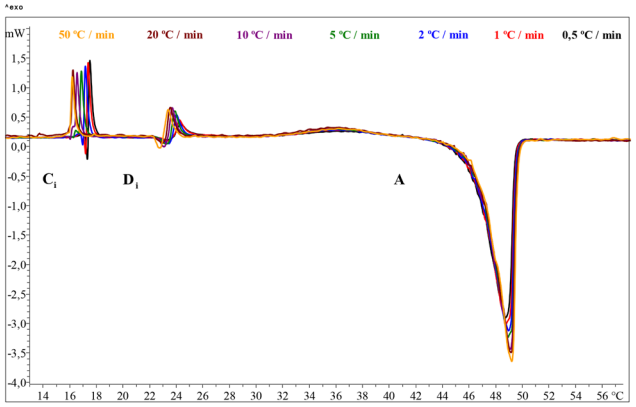

Fig. 4 Overlapping DSC thermograms of ubiquinone at a heating rate of 1 °C min^{-1} from 0 °C to 70 °C (method B, step 4). The heating rates of the previous cold crystallization step (Fig. 3) are shown in the figure for clarity. Enlarged view from 14 °C to 57 °C. Ci refers to form C, crystallized according to the heating rate of the cold crystallization applied and Di refers to form D, crystallized according to the respective melting of form C.

crucibles at 25 °C without any mechanical treatment in order to avoid induced polymorph transitions and analyzed immediately by XRPD (Fig. 5). The two samples show essentially the same pattern but with a different degree of crystallinity, which strongly suggests that the exothermic phenomenon can be considered a thermal rearrangement of form A with an increase of the degree of crystallinity.

Stage 2: study of endothermic/exothermic thermal events above 0 °C at different heating rates. DSC experiments have been carried out applying different cycling methods with different heating rates after a common cold crystallization phenomenon observed between −100 °C and 0 °C (see ESI† Table S2 and method C). A heating rate of 5 °C min^{-1} was chosen for the cold crystallization step from −100 °C to 0 °C. Then, variable heating rates from 0 °C to 70 °C were applied and the same crystalline rearrangement–melting–crystallization consecutive phenomena were observed as before, shifting to a higher temperature when decreasing the heating rate (Fig. 6). This set of experiments supports the hypothesis of kinetics-

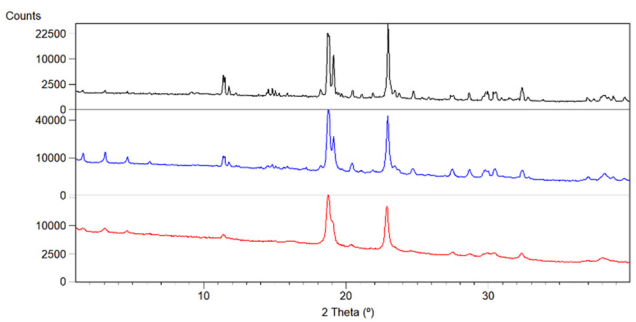

Fig. 5 XRPD comparative diffractograms: in the 1st experiment, heating until 28 °C (red), in the 2nd experiment, heating until 40 °C (blue), and ubiquinone bulk powder (black) (see also Fig. S4† for further details).

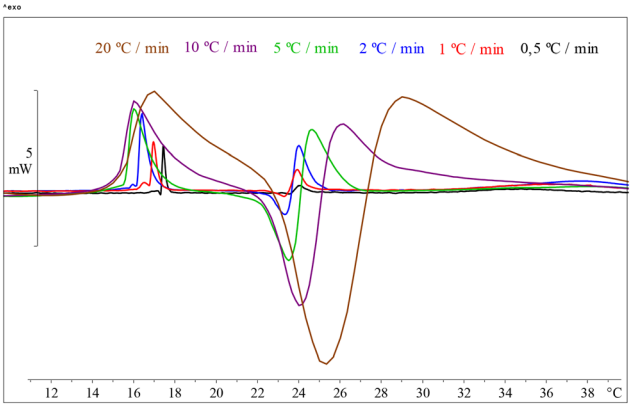

Fig. 6 Overlapping DSC thermograms of ubiquinone after cold crystallization at a 5 °C min^{-1} heating rate of the amorphous form, from 0 °C to 70 °C at different heating rates (method C, step 4). Enlarged view from 12 °C to 37 °C. The DSC thermogram at a heating rate of 50 °C min^{-1} is not represented for clarity.

dependent conformational forms suggested in stage 1. High heating rates (20 and 50 °C min^{-1}) prevent the observation of the complex consecutive thermal events, instead a broad exothermic phenomenon is registered. Usually, high heating rates reduce the resolution of very close thermal events as it is the case.

Two more experiments were carried out in order to study whether the cold crystallization process affects the postulated crystalline rearrangement–melting–crystallization consecutive phenomena of polymorphs above 0 °C using a heating rate of 1 °C min^{-1} and 50 °C min^{-1} for the previous cold crystallization step from −100 °C to 0 °C (Fig. S5 and S6,† respectively) showing the same behavior as described above in both cases.

It is important to mention that the melting point onsets of forms C and D shifted to lower values when the heating rate was increased. Thus, in order to discard any instrumental shift of the melting point due to the change in the heating rate, DSC control experiments were carried out with ubiquinone bulk powder (form B) analyzing the sample at different heating rates: 0.5, 1, 10, and 20 °C min^{-1} (see ESI† Fig. S7 and method A). The results revealed the expected shift of the melting point onset for a unique form to high temperatures when the heating rates are increased. This is what usually occurs for any crystalline material and confirms that the different onsets observed after the quenching-from-the-melt experiments can be related to a conformational polymorphism hypothesis governed by the kinetic crystalline rearrangement, discarding any instrumental effect.

In order to complete the characterization of the polymorphism landscape of CoQ10, the relationship between polymorphs A and B was determined based on the experimental melting data values obtained at a heating rate of 10 °C min^{-1}. Thus, a monotropic relationship between forms A and B can be deduced (melting point form A = 45 °C, ΔH_A= 104.5 J g^{-1}; melting point form B = 51 °C, ΔH_B= 105.4 J g^{-1}).[22] The most complex thermal behavior for forms C and D precluded a similar analysis.

Polymorphism of ubiquinol

Ubiquinol exists in two anhydrous forms according to the patent published in 2015 (ref. 24) that reported DSC experiments (at heating rate of 1 °C min^{-1}) of both polymorphs: form A shows an endothermic peak at 48 °C and form B at 52 °C, neither enthalpies of fusion nor DSC thermograms were reported. Now, we have crystallized form A in ACN and used form B from commercial sources and characterized them by DSC (Fig. S8 and S10†), TGA (Fig. S9 and S11†) and XRPD (Fig. S12†).

Analysis of the enthalpy of melting indicates that forms A and B are enantiotropically related according to the heat-of-fusion rule since the higher enthalpy of fusion corresponds to the lower melting point form: the melting point of form A at 47.0 °C with an associated heat of 118.97 J g^{-1} and the melting point of form B at 50.7 °C with an associated heat of 94.51 J g^{-1}. Thus, the transition temperature between the enantiotropic pair was estimated using the theoretical approach by Yu[25] based on the melting data of both polymorphs (see the ESI† for further details, eqn (S1)). The theoretical value obtained by following this calculation was 34.2 °C.

Thermal analysis of ubiquinol quenched from the melt

In the second part of this work, ubiquinol was studied in the same manner in order to check if it shares a similar behaviour to ubiquinone, its oxidized counterpart. Thus, commercial powder ubiquinol (form B) was heated at 10 °C min^{-1} under dry nitrogen until 300 °C. Since no decomposition in terms of loss in weight was observed after the melting of ubiquinol (Fig. S8 and S9†), a quenching-from-the-melt experiment was conducted, revealing the presence of polymorphism (Fig. S13†). In this sense, after quenching from the melt, the amorphous phase was detected, showing a glass transition at −64.5 °C with a ΔC_p of 0.522 J g^{-1} K^{-1} when heated at 5 °C min^{-1} according to method B-4. In a similar fashion to ubiquinone, DSC experiments have been carried out applying different methods at different heating rates after a common quenching-from-the-melt cooling rate program (see ESI† Table S3 and method B) to study the polymorphism of ubiquinol observed in the first quenching (Fig. S13†). Similar to ubiquinone, cold crystallization occurs after the glass transition and they both shift to higher temperatures when the heating rate is increased indicating their kinetically controlled nature (Fig. S14†). In this case, the amorphous form of ubiquinol is kinetically more stable than that of ubiquinone (glass transition at −64.5 °C *versus* −71.65 °C, respectively), showing incomplete cold crystallization when high heating rates (10, 20, and 50 °C min^{-1}) were applied. As a result, the completion of the cold crystallization for these heating rates was observed in the next step, when it was heated at 1 °C min^{-1} between 0 °C and 70 °C, (Fig. S15†). As a consequence of varying heating rates on the previous cold crystallization process, different behaviors were observed during the DSC experiment above 0 °C, suggesting three main endothermic/exothermic overlapping processes, (Fig. 8). In particular, with low heating rates (0.5, 1, and 2 °C min^{-1}), a phase (named form C) was crystallized. With medium heating rates (10

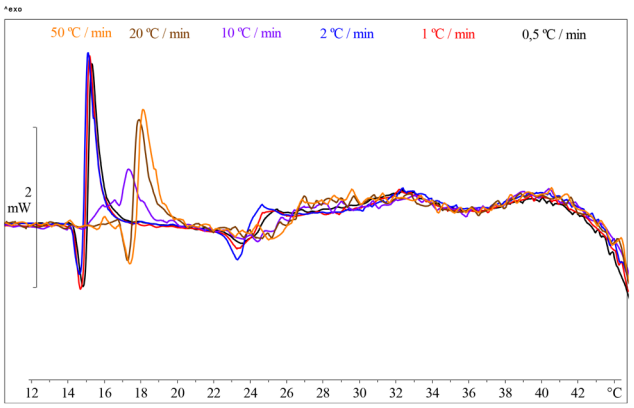

Fig. 7 Overlapping DSC thermograms of ubiquinol at a heating rate of 1 °C min^{-1} from 0 °C to 70 °C (method B, step 4). The heating rates of the previous cold crystallization step (Fig. S14†) are shown in the figure for clarity. Enlarged view from 12 °C to 44 °C.

°C min^{-1}), another phase (named form D) was produced, and finally, with high heating rates (20 and 50 °C min^{-1}) another phase (named form E) crystallized (Fig. 7). We postulate that all three forms subsequently transform into form A with a low degree of crystallinity through a melting–crystallization overlapped phenomena followed by (in a similar manner to ubiquinone) a final thermal rearrangement.

Similar to ubiquinone, the subtle differences in the thermal behavior of the postulated C, D and E forms suggest that the different heating rates during the cold crystallization process affect the crystallization events leading to the formation of different, or at least more ordered, solids forms, as mentioned above, which can be related to conformational polymorphs with similar physical properties.

Since X-ray powder diffraction (XRPD) is a valuable tool in the assessment of crystal disruption resulting from various processing stresses as quenching[2,3] and aiming to further characterize the polymorphism of ubiquinol observed by DSC in quenching-from-the-melt experiments, XRPD analysis in transmission configuration at a variable temperature was conducted. Unfortunately, due to the limitations of the temperature control by our instrument cryostat only a 6 °C min^{-1} heating/cooling rate experiment could be performed. Once ubiquinol (form B) was melted in the capillary, it was cooled down at a rate of 6 °C min^{-1} until −100 °C and subsequently heated up to 70 °C at a rate of 6 °C min^{-1}, measuring a diffractogram periodically. (Fig. 9 (up), shows with colored dots, the different temperature values where XRPD was measured during the second heating process. See also Fig. S19 and S20†). The results during the reheating process show that at 20 °C form C (Fig. S22†) was detected (with low crystallinity), and finally converted into form A (Fig. S24†) (peaks at 18.9 and 20.2 2θ are particularly useful to differentiate between the three forms mentioned and are highlighted in Fig. 9 (down)). Thus, XPRD data provided more evidence to reinforce the hypothesis previously postulated about the presence of intermediate crystal phases. Unfortunately, in spite of significant efforts during our study, no structural information could be generated to corroborate our rational conclusions based on a rigorous analysis of a large set of DSC experiments. However, experimental work is

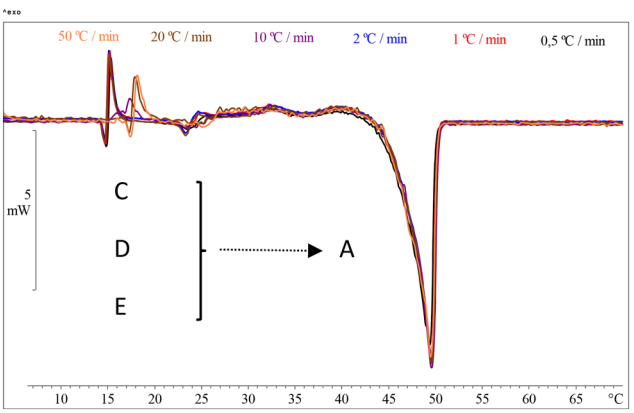

Fig. 8 Overlapping DSC thermograms of ubiquinol at a heating rate of 1 °C min^{-1} from 0 °C to 70 °C (method B, step 4). The heating rates of the previous cold crystallization step (Fig. S14†) are shown in the figure for clarity. Enlarged view from 7 °C to 70 °C.

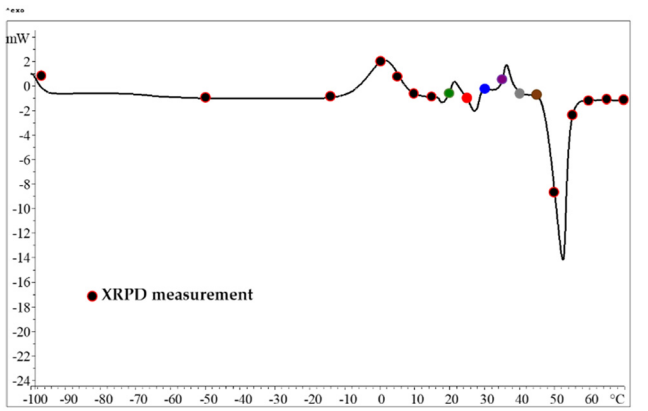

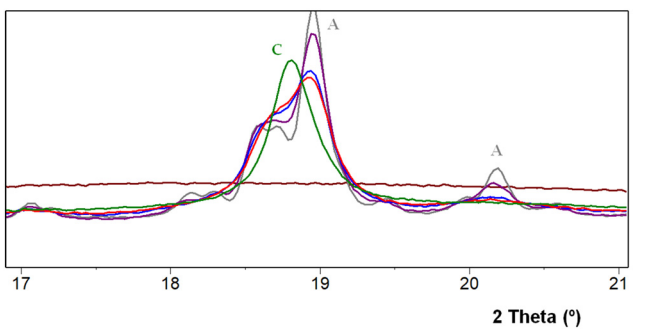

Fig. 9 (Up) DSC thermogram of recrystallized-from-the-melt ubiquinol at a heating rate of 6 °C min^{-1} from −100 °C to 70 °C (method G, step 3). Temperature variable XRPD measurements are highlighted according to the thermal evolution of the solid. (Down) Comparative XRPD diffractograms of the temperature evolution during the reheating process at 20 °C (green, form C), 25 °C (red, thermal rearrangement), 30 °C (blue, thermal rearrangement), 35 °C (purple, form A), 40 °C (grey, form A), and finally 45 °C (brown, liquid). Enlarged view from 17 to 21° 2θ.

currently being carried out in our laboratory to obtain good quality single crystals.

Conclusions

New polymorphs, low crystalline forms and amorphous phases of the oxidized and reduced forms of Coenzyme Q10 have been detected by means of DSC using a variety of experimental conditions that has allowed us to obtain a deeper insight into the effect of kinetics on the cold crystallization of several conformational polymorphs that were previously unreported. Both ubiquinone and ubiquinol are very flexible compounds[26] with a chain of 10 isoprenoid units with all double bonds in the *E* configuration. We postulate that the highly hydrophobic isoprenoid chains are able to pack in the solid state in many different ways of almost equivalent energy, providing a plausible explanation to the observed polymorphism and enthalpic reorganization in both compounds. Unfortunately, single crystals of the required quality for SCXRD analysis have not been obtained despite considerable experimental efforts.

Data availability

The data supporting this article (detailed analysis conditions, NMR, DSC, TGA, and PXRD diagrams, Fig. S1 to S24†) have been included as part of the ESI.†

Author contributions

The manuscript was collaboratively written by all authors, who have approved the final version. Conceptualization: RB and RP; methodology: RB, RP, LB and DdS; validation: RP and RB; formal analysis: LB, RB, and RP; investigation: RB, RP, LB and DdS; resources: RP and RB.; data curation: RB and LB; writing – original draft preparation: LB, RB, and RP; writing – review and editing: RB and RP; supervision: RP; project administration: RP; funding acquisition: RP.

Conflicts of interest

The authors declare no conflict of interest.

Acknowledgements

The authors thank the Unitat de Difracció de Raigs X and Unitat de Ressonància Magnètica Nuclear of the Centres Científics i Tecnològics, University of Barcelona for access to their facilities. This research was supported by the Research Project of MICIU/AEI of Spain (project PID2023-146632OB-I00).

Notes and references

1 *Physical Characterization of Pharmaceutical Solids*, ed. H. G. Brittain, 1st edn, 1995, CRC Press, DOI: 10.1201/9780367802967.
2 G. P. Stahly, *Cryst. Growth Des.*, 2007, **7**, 1007–1026.
3 L. Fabian and A. Kalman, *Acta Crystallogr., Sect. B: Struct. Sci.*, 2004, 60547–60558.
4 R. Prohens, R. Barbas and M. Font-Bardia, *Cryst. Growth Des.*, 2020, **20**, 4238–4242.
5 D. Dey, S. P. Thomas, M. A. Spackman and D. Chopra, *Chem. Commun.*, 2016, **52**, 2141–2144.
6 T.-W. Shyr, C.-H. Tung, W.-S. Cheng and C.-C. Yang, *J. Polym. Res.*, 2013, **20**, 186.
7 J. Henricks, M. Boyum and W. Zheng, *J. Therm. Anal. Calorim.*, 2015, **120**, 1765–1774.
8 K. Ishino, H. Shingai, Y. Hikita, I. Yoshikawa, H. Houjou and K. Iwase, *ACS Omega*, 2021, **6**, 32869–32878.
9 Y. Tsujimoto, T. Sakurai, Y. Ono, S. Nagano and S. Seki, *J. Phys. Chem. B*, 2019, **123**, 8325–8332.
10 S. Sampath, A. A. Boopathia and A. B. Mandal, *Phys. Chem. Chem. Phys.*, 2016, **18**, 21251.
11 J. A. Baird, B. Van Eerdenbrugh and L. S. Taylor, *J. Pharm. Sci.*, 2010, **99**, 3787–3806.
12 M. Arenas-Jal, J. M. Suñé-Negre and E. García-Montoya, *Compr. Rev. Food Sci. Food Saf.*, 2020, **19**, 574–594.
13 Y. Liang, D. Zhao, Q. Ji, M. Liu, S. Dai, S. Hou, Z. Liu, Y. Mao, Z. Tian and Y. Yang, *EClinicalMedicine*, 2022, **52**, 101602–101623.
14 D. Mantle and A. Dybring, *Antioxidants*, 2020, **9**, 386–398.
15 W. V. Judy, *Integr. Med.*, 2021, **20**, 24–28.
16 L. Bofill, D. de Sande, R. Barbas and R. Prohens, *Cryst. Growth Des.*, 2020, **20**, 5583–5588.
17 H. Katsikas and P. Quinn, *J. Bioenerg. Biomembr.*, 1983, **15**, 67–79.
18 S. L. Price, *Acta Crystallogr., Sect. B: Struct. Sci., Cryst. Eng. Mater.*, 2013, **69**, 313–328.
19 A. J. Briard, M. Bouroukba, D. Petitjean, N. Hubert and M. Dirand, *J. Chem. Eng. Data*, 2003, **48**, 497–513.
20 K. V. Gataullina, M. A. Ziganshin, I. I. Stoikov, A. E. Klimovitskii, A. T. Gubaidullin, K. Suwińska and V. V. Gorbatchuk, *Cryst. Growth Des.*, 2017, **17**, 3512–3527.
21 Y. Zhao, Y. H. Sun, Z. Y. Li, C. Xie, Y. Bao, Z. J. Chen, J. B. Gong, Q. X. Yin, W. Chen and C. Zhang, *J. Solution Chem.*, 2013, **42**, 764–771.
22 A. Burger and R. Ramberger, *Microchim. Acta*, 1979, **72**, 259–271.
23 N. S. Trasi and S. R. Byrn, *AAPS PharmSciTech*, 2012, **13**, 772–784.
24 H. Kawachi, S. Kitamura and Y. Udea, *US Pat.*, US2015/0284311A1, 2015.
25 L. Yu, *J. Pharm. Sci.*, 1995, **84**, 966–974.
26 E. D. Tekin and S. Erkoc, *Mol. Simul.*, 2010, **36**, 763–771.

